nature cell biology

# Loss of centrosome integrity induces p38–p53–p21-dependent G1–S arrest

Keith Mikule[1,4,5], Benedicte Delaval[1,5], Philipp Kaldis[2], Agata Jurcyzk[1], Polla Hergert[3] and Stephen Doxsey[1,6]

**Centrosomes organize the microtubule cytoskeleton for both interphase and mitotic functions. They are implicated in cell-cycle progression but the mechanism is unknown. Here, we show that depletion of 14 out of 15 centrosome proteins arrests human diploid cells in G1 with reduced Cdk2–cyclin A activity and that expression of a centrosome-disrupting dominant-negative construct gives similar results. Cell-cycle arrest is always accompanied by defects in centrosome structure and function (for example, duplication and primary cilia assembly). The arrest occurs from within G1, excluding contributions from mitosis and cytokinesis. The arrest requires p38, p53 and p21, and is preceded by p38-dependent activation and centrosomal recruitment of p53. p53-deficient cells fail to arrest, leading to centrosome and spindle dysfunction and aneuploidy. We propose that loss of centrosome integrity activates a checkpoint that inhibits G1–S progression. This model satisfies the definition of a checkpoint in having three elements: a perturbation that is sensed, a transducer (p53) and a receiver (p21).**

The centrosome is primarily known for its microtubule organizing function. However, centrosomes contain hundreds of proteins with diverse functions suggesting roles in numerous cellular activities[1]. Animal cell centrosomes are structurally complex organelles comprised of two microtubule–based centrioles surrounded by a protein matrix (pericentriolar material, PCM) and other structural elements. Similarly to DNA replication, the centrosome duplication process occurs once per cell cycle, is semi-conservative, initiates in G1 and is controlled by the same cyclin-dependent kinases[2,3]. A single interphase centrosome yields two mature centrosomes at mitosis, which participate in organization of bipolar spindles and segregation of chromosomes. Most human carcinomas are characterized by aberrant centrosomes[4,5], which are thought to organize dysfunctional spindles and contribute to genetic instability.

Recent studies indicate that centrosomes have a role in cytokinesis and that disruption of this function is associated with cell-cycle arrest. For example, when centrosomes are removed[6,7] or disrutped[8], cytokinesis is impaired and cells arrest in G1. In contrast, cell-cycle progression is not affected in cells with extra centrosomes, extra nuclei or after pharmacological disruption of cytokinesis[9,10]. These results indicate that centrosome-associated G1 arrest occurs only when centrosomes are absent or compromised. Other studies demonstrate that progression from G1 into S phase requires binding of cell-cycle regulatory molecules to centrosomes[1,11]. However, little is known about how centrosomes contribute to the G1 to S phase transition.

## RESULTS

### Depletion of centrosome proteins reduces their centrosome levels and induces G1 arrest

To address the role of centrosomes in cell-cycle progression, we targeted fifteen centrosome proteins for depletion using small-interfering RNAs (siRNAs). We used human diploid epithelial cells (RPE-1) and confirmed results with three other human diploid cell lines (see Methods). Targeted proteins included integral centrosome and/or centriole components, as well as regulatory proteins that affect centrosome function. Three non-centrosomal proteins served as negative controls (including the intermediate filament protein lamin and the actin-associated protein zyxin). Indirect immunofluorescence staining of individual cells revealed a consistent reduction in the centrosome-associated fraction of all targeted centrosome proteins (Fig. 1a and see Supplementary Information, Fig. S1a–c), even though many have significant cytoplasmic fractions. Western blots of whole-cell lysates showed reduction in the global level of targeted proteins (see Supplementary Information, Figs S1d).

Depletion of 14–15 centrosome proteins induced G1 arrest (Fig. 1). Cells failed to reach confluency, exhibited a low mitotic index, did not progress into S phase (BrdU-negative, Fig. 1b) and showed reduced reactivity for the proliferating antigen Ki-67 (Fig. 1c)[12]. Flow cytometry analysis of pericentrin-depleted cells revealed a small increase in the G1 peak (2N DNA content) over controls (Fig. 1d) and a concomitant decrease in the G2 peak was observed. Similar changes were observed for depletion of the centrosome proteins centriolin and PCM1, but not

[1]Program in Molecular Medicine, University of Massachusetts Medical School, Worcester, Massachusetts 01605, USA. [2]National Cancer Institute, Fredrick, Maryland 21702, [3]Wadsworth Center, Albany, New York 12201, USA. [4]Current address: ArQule Biomedical Institute, Inc., Norwood, Massachusetts 02062,USA.
[5]These authors contributed equally to this work.
[6]Correspondence should be addressed to S.D. (email: Stephen.Doxsey@umassmed.edu)

Received 31 August 2006; accepted 14 December 2006; published online 24 December 2006; DOI: 10.1038/ncb1529

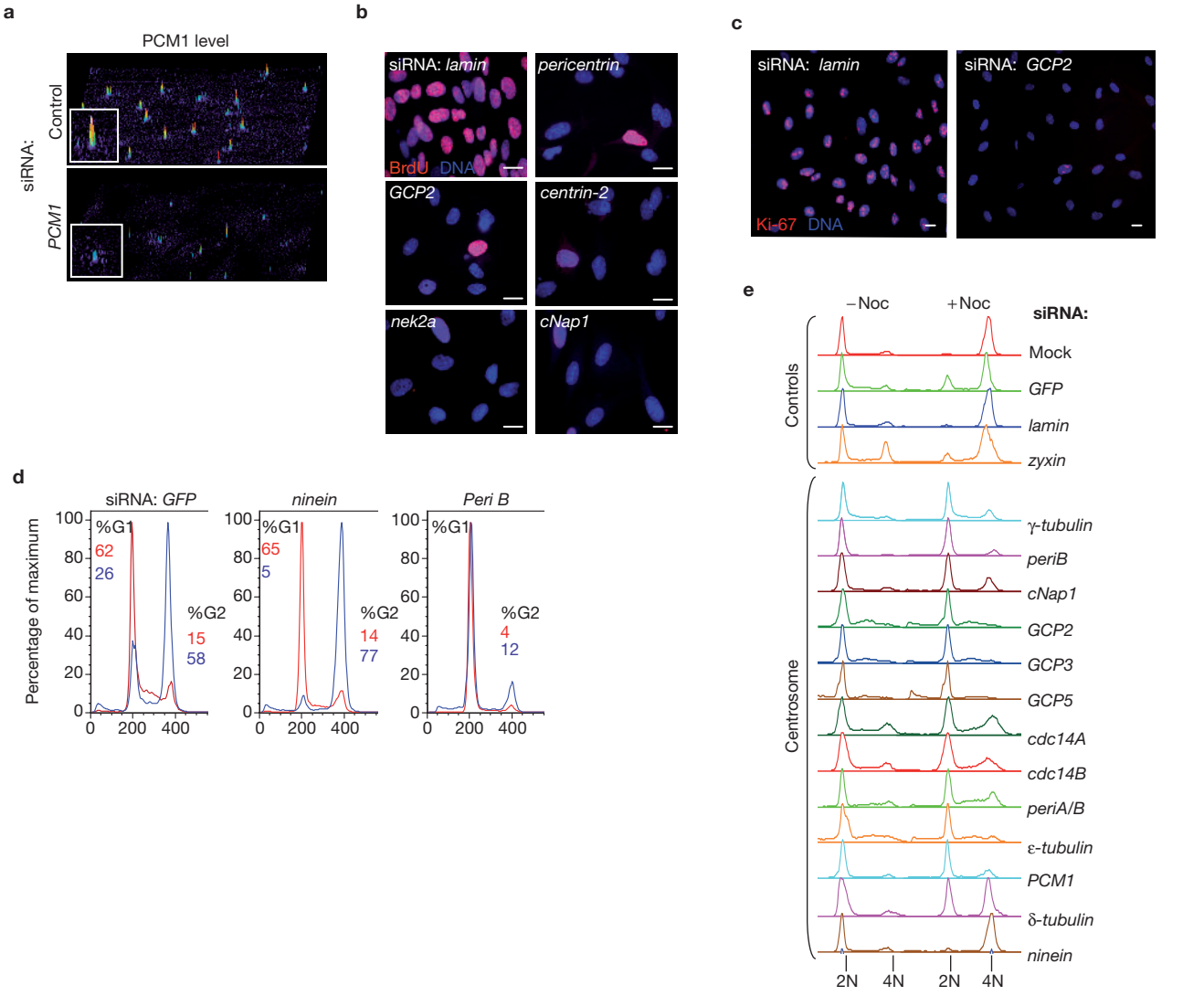


**Figure 1** siRNA-mediated centrosome protein depletion triggers G1 arrest. (**a**) Semi-quantitative pixel intensity profiles of centrosomes produced from optically sectioned (*z*-axis) fluorescence images show depletion of centrosomal PCM1 (inset shows enlarged pixel intensity profile of centrosome). Colour indicates staining intensity. Profiles for other proteins are shown in the Supplementary Information, Fig. S1. (**b**) BrdU incorporation (16 h pulse) in siRNA-treated (72 h) cells, as indicated. (**c**) Immunoflorescence microscopy images showing that Ki-67 staining is not present in nuclei of most *GCP2* siRNA-treated cells (72 h) but is present in cycling control cells (*lamin*). (**d**) Flow cytometry profiles of cells labelled with propidium iodide. Cells were treated with indicated siRNAs for 72 h without (red, DMSO) and with (blue) nocodazole for the final 12 h (>10000 cells per profile). More profiles are shown in the Supplementary Information, Fig. S2a. (**e**) Flow cytometry profiles of cells treated with the indicated siRNAs for 72 h then with DMSO (– noc) or nocodazole (+ noc) for the final 12 h. Profiles are representative of three experiments (>5000 cells per profile). The scale bar represents 10 μm in **b** and **c**.

for ninein (data not shown, Fig. 1d). To highlight cell-cycle differences, cells were treated with nocodazole to depolymerize microtubules, activate the spindle assembly checkpoint and accumulate cells in G2–M with 4N DNA content. Remarkably, nearly all centrosome-depleted cells were retained in the G1 peak with 2N DNA content and did not shift to the G2–M peak, whereas control cells did (Fig. 1d, e). Depletion of all centrosome proteins but one induced G1 arrest (Fig. 1b, e). Cells treated with siRNAs targeting control RNAs or *ninein*[13] continued to cycle normally. *Ninein* depletion had no effect on cell-cycle progression despite the fact that it was significantly reduced at centrosomes following treatment with two independent siRNAs (see Supplementary Information, Fig. S1c). We did not determine whether the lack of cell-cycle arrest in *ninein*-depleted cells (and the partial arrest in *δ-tubulin*-depleted cells, Fig. 1e) was due to insufficient protein reduction, a lack of function in this pathway or the presence of proteins with redundant functions (for example, ninein-like protein[14]). Targeted centrosome proteins were localized to different centrosomal sites including PCM, centrioles, mother centriole or subdistal appendages, suggesting that a single centrosome substructure was not involved in the arrest.

## G1 arrest is specifically suppressed by re-expression of the target protein

In addition to several control RNAs targeted in our siRNA experiments, we performed other experiments to demonstrate that the cell-cycle arrest

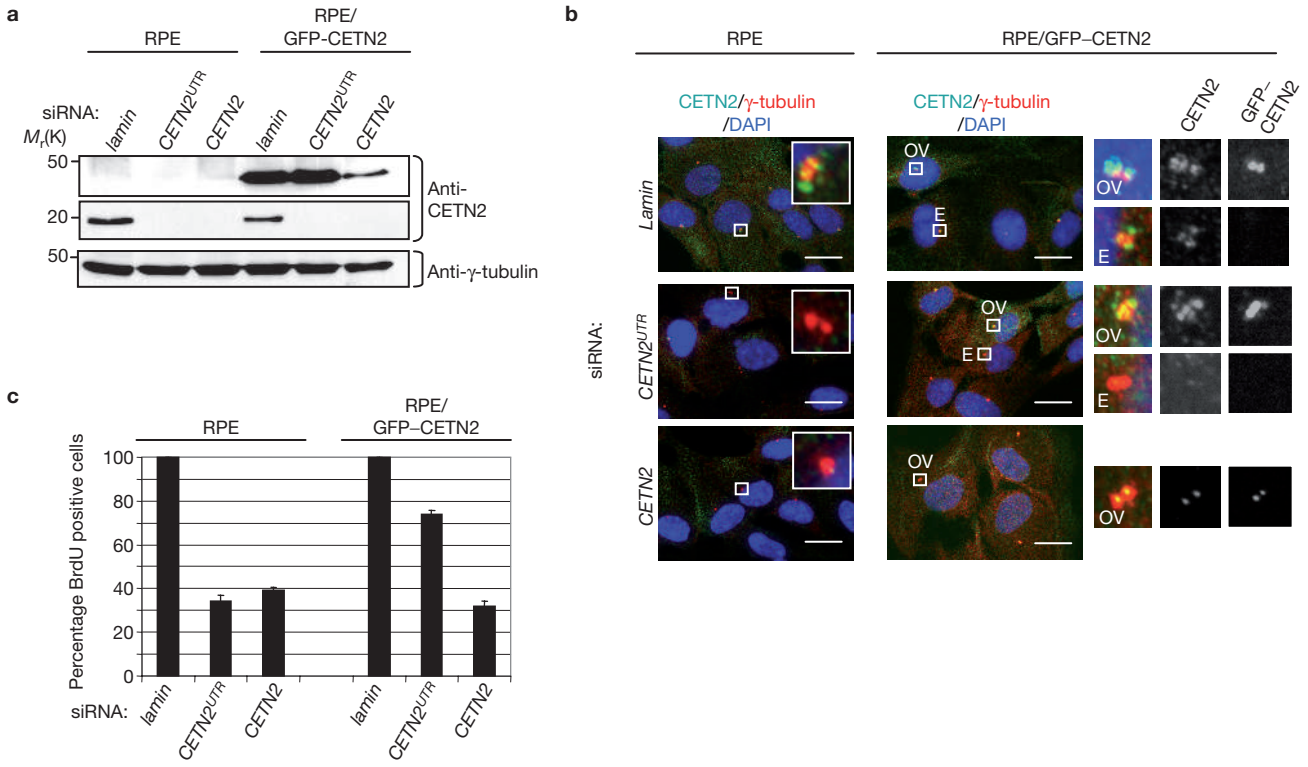


**Figure 2** G1 arrest can specifically be suppressed by overexpression of the target protein. **(a)** Western blots from RPE and RPE/ GFP–Cetn2 cells treated with siRNAs as indicated and probed with centrin antibody (20H5) to show endogenous (middle panel) and overexpressed (upper panel) centrin. Lamin, control. *Cetn2*$^{UTR}$ siRNA targets only endogenous *Cetn2*, *Cetn2* siRNA targets both endogenous *Cetn2* and GFP–*Cetn2*. γ-tubulin staining demonstrates equivalent loading conditions. (**b**) Immunofluorescence microscopy images taken from siRNA-treated RPE cells (72 h) show reduced level of endogenous Cetn2 protein (green) at the centrosome with both *Cetn2*$^{UTR}$ siRNA and *Cetn2* siRNA, when compared with normal levels obtained with *lamin* siRNA (insets show enlargements of indicated centrosomes). Images taken from siRNA-treated RPE overexpressing GFP–Cetn2 (right columns) show reduced level of overexpressed GFP-Cetn2 at the centrosome with *Cetn2* siRNA but not with *Cetn2*$^{UTR}$ siRNA. Enlargements of centrosomes from an overexpressing cell (ov, top inset from each picture) and a non overexpressing cell in the same field (E, endogenous, bottom inset) are shown on the right. γ-tubulin, centrosome marker (red). The scale bar represents 10 μm. (**c**) Quantification of BrdU incorporation (16 h pulse) in siRNA-treated RPE and RPE cells overepressing GFP-Cetn2. Average of three independent experiments ± s.e.m. is shown.

was specific for depletion of centrosome proteins. We first tested whether G1 arrest could be suppressed by re-expression of the targeted RNA. An siRNA that targeted the 5′-untranslated region (UTR) of endogenous *centrin 2*, but did not target ectopically expressed GFP–centrin 2, was used (Fig. 2). As expected, the UTR-directed siRNA efficiently depleted endogenous *centrin 2* but not GFP–centrin 2, as determined by immunoblotting and immunofluorescence microscopy (Fig. 2a, b). Cell-cycle analysis demonstrated that control cells depleted of endogenous *centrin 2* arrested, whereas most cells ectopically expressing GFP–centrin 2 continued to cycle (Fig. 2c). When GFP–centrin 2-expressing cells were treated with a siRNA targeting both endogenous *centrin 2* and *GFP–centrin 2* (Fig.2b), G1 arrest was induced (Fig. 2a–c). This demonstrated that centrin 2 was specifically required for cell-cycle progression and suggested that centrosome localization was important for this function (GFP-tagged centrin localized to centrosomes, data not shown).

In a separate experiment, cells were kept under sustained cell-cycle arrest (for 10 days) by repeated treatment with siRNAs targeting *pericentrin* (see Supplementary Information, Fig. S2b). When siRNAs were washed out, cells resumed cycling only after pericentrin was re-expressed and localized properly to centrosomes. These two 'rescue' experiments demonstrate that centrosome protein depletion induces a specific and reversible G1 arrest.

## Mislocalization of centrosomal pericentrin by a dominant-negative pericentrin domain induces G1 arrest

To more specifically test whether loss of protein from centrosomes induced G1 arrest, we expressed the carboxyl-terminus of pericentrin (Peri$^{CT}$), which functions in a dominant-negative manner by disrupting the centrosome-bound fraction of endogenous pericentrin[15]. Most cells expressing RFP-tagged Peri$^{CT}$ were unable to incorporate BrdU after a 24-h pulse, whereas those expressing RFP alone were mostly BrdU-positive (Fig. 3a, 17% versus 98% BrdU+, $n$ = 50 cells). This experiment demonstrates that cell-cycle arrest can be induced by ectopic expression of a centrosome protein, in addition to centrosome protein depletion.

Other studies have shown that a G1-like arrest can be induced by microinjection of PCM1 antibodies into mouse embryos[16] or centriolin antibodies into *Xenopus* embryos[8]. Thus, G1 arrest can be induced by centrosome protein depletion, overexpression or antibody binding in both cultured cells and multicellular organisms. Cell-cycle arrest by three independent centrosome-targeting methods in three different experimental systems argues that this phenomenon is specific for centrosomes.

## G1 arrest can be induced in postmitotic cells from within G1

We next examined whether G1 arrest was a consequence of mitotic defects. In the experiment shown in Fig. 3a, cells were identified by time-lapse

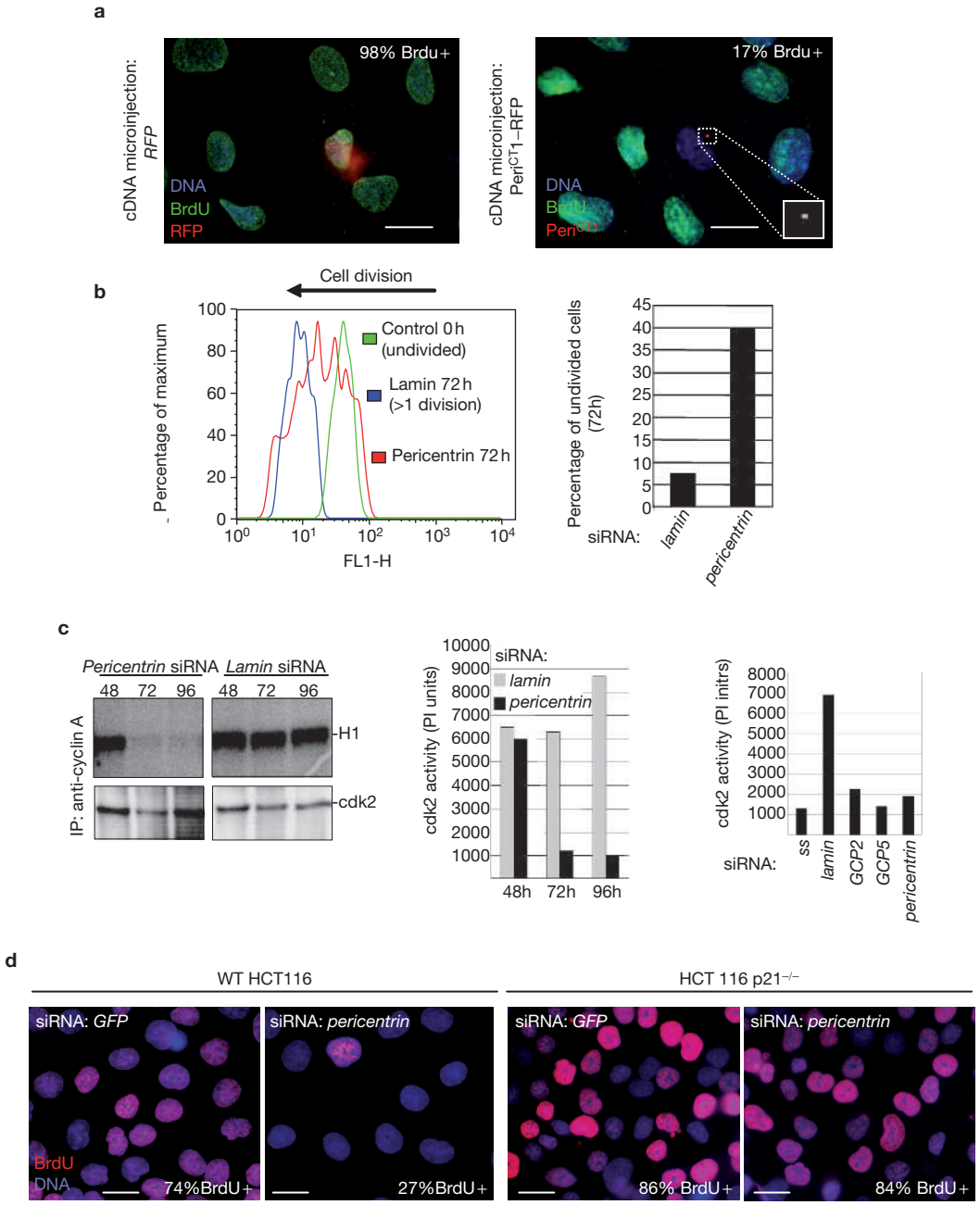


**Figure 3** G1 arrest can be induced from within G1, occurs in late G1 with reduced Cdk2–cyclin A activity and is suppressed by deletion of the *p21* gene. (**a**) Cells microinjected in late telophase or early $G_1$ with plasmids encoding either the Peri$^{CT}$–RFP or RFP alone, as indicated. BrdU incorporation was determined 24 h later (inset shows enlargement of the centrosome of a Peri$^{CT}$–RFP expressing cell with no BrdU incorporation, nonexpressing cells in the same field incorporate BrdU). Quantification shows that most Peri$^{CT}$–RFP expressing cells do not incorporate BrdU. (**b**) Cells accumulated in G1–G0 with low serum were loaded with a fluorescent probe to track population doublings then treated with the indicated siRNAs to deplete proteins within G1. Flow cytometry was performed on one set of samples before addition of siRNA to serve as a nondivided control population (green trace). Other samples were treated with indicated siRNAs for 72 h. Serum was added during the last 24 h to induce cycling. Flow cytometry profiles show that a population of *pericentrin* siRNA-treated cells (arrested by serum starvation at the time of transfection) retains the original label showing that cells did not divide at all (left, red trace within green) and others seemed to arrest after one or two divisions (additional peaks due to the fact that 24 h after serum starvation some cells are not yet arrested). Few *lamin*-depleted control cells were found in the undivided peak; most divided two or three times (blue trace). The histogram shows percentage of cells that did not divide. All results are representative of three experiments. (**c**) Cyclin A immunoprecipitations and cdk2 immunoprecipitation–kinase assays from cells treated with indicated siRNAs. Autoradiographs of histone H1 phosphorylation from cyclin A immunoprecipitations and immunoblots for cdk2 are shown. Results representative of three experiments. The histograms show quantification of histone H1 phosphorylation by cdk2 after normalizing for cdk2 levels. PI, phosphorimager units; ss, serum starved 0.25% serum. (**d**) BrdU incorporation (16 h pulse) in HCT116 and HCT116 *p21*$^{-/-}$ cells as indicated following 60 h siRNA-treatment as indicated. The scale bars represent 10 μm in **a** and **d**.

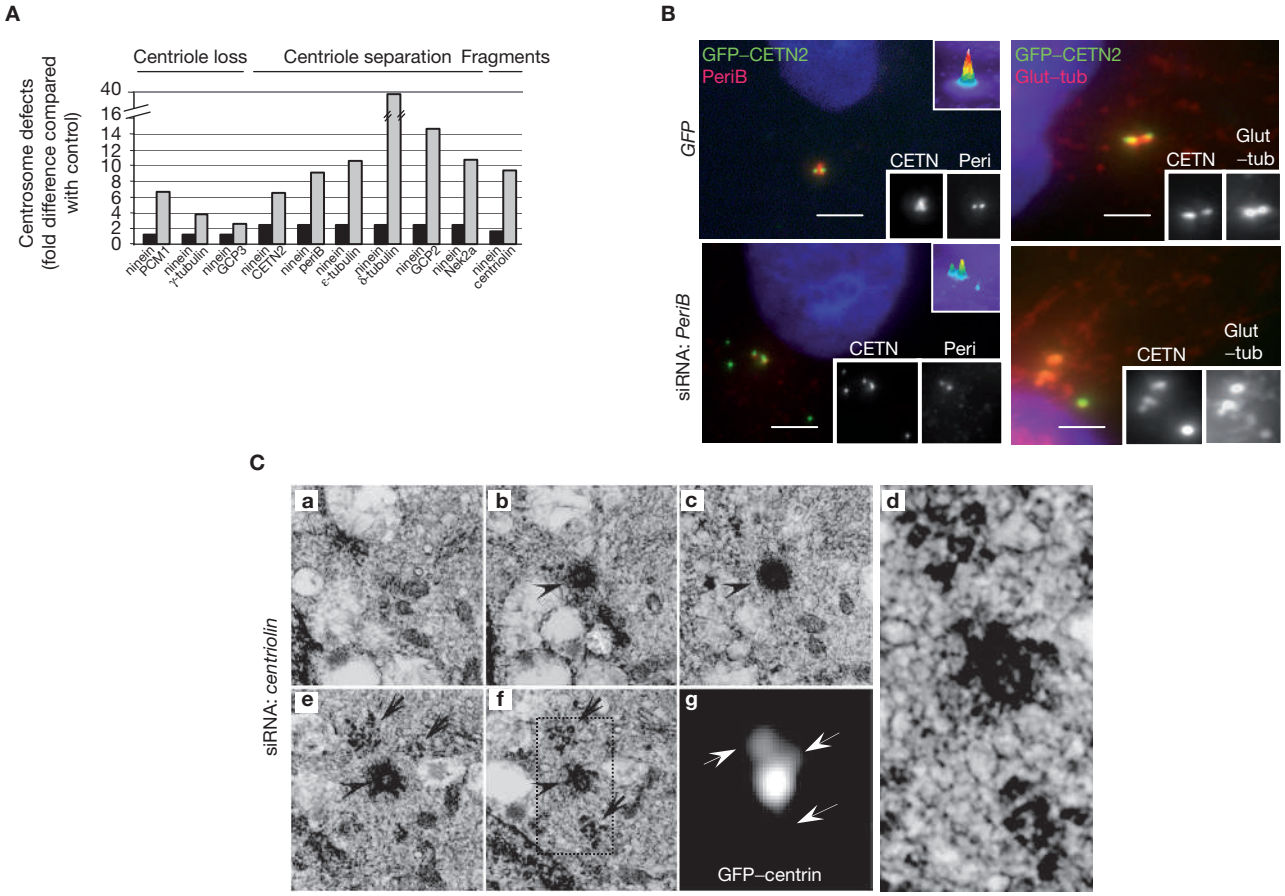


**Figure 4** G1 arrested cells show defects in centrosome structure and organization. (**A**) Quantification of cells with defects in centrosome structure and organization following siRNA treatment for the indicated proteins (fold difference normalized to GFP and compared to ninein, see Methods). The results are representative of two experiments (see Supplementary Information, Fig. S3). (**B**) Immunofluorescence microscopy images of seemingly incomplete centrosome-like structures that stain for centriole markers (centrin, CETN and polyglutamylated tubulin; Glut-tub) but not for PCM markers (pericentrin, peri; or γ-tubulin) in RPE-1 cells stably expressing GFP–centrin2 and depleted of the indicated centrosome proteins. The scale bars represent 2 μm. (**C**) Correlative electron microscopy of incomplete centrosome-like structures in serial sections (**a**–**e**) observed by immunofluorescence microscopy (**d**, arrows) and the two parent centrioles (arrowheads indicate daughter centriole in **b** and **c** and mother centriole in **d** and **e**). Enlargement of box in **e** shows mother centriole (**g**, centre) and incomplete centrosome-like structures (above and below).

imaging as they completed cytokinesis[17], and were then microinjected with a plasmid containing the dominant-negative pericentrin construct to induce protein expression in G1. As described earlier, G1-stage pericentrin-expressing cells never entered S-phase, whereas control cells continued to cycle, demonstrating that arrest was induced in postmitotic cells (Fig. 3a). In a second strategy, cells were accumulated in G0–G1 by serum withdrawal then treated with siRNAs to deplete *pericentrin*. Subsequently, bulk cellular proteins were labelled with a fluorescent dye (CFDA-SE), the total amount of which is halved after each cell division[18], and serum was added to release cells from the G0–G1 arrest. Nearly all control cells divided about three times, whereas ~40% of pericentrin-depleted cells did not divide at all during the same time period (Fig. 3b). These two independent approaches demonstrate that G1 arrest can be induced from within G1, and that perturbation of mitotic events, such as spindle function and cytokinesis, are not required to trigger the arrest.

## G1 arrest occurs concomitant with reduced Cdk2–cyclinA activity and requires p21

To more accurately determine the cell-cycle stage and molecular mechanism of the G1 arrest, we examined the levels and activity of Cdk–cyclin complexes. Immunoprecipitations from pericentrin-depleted cells showed that Cdk2–cyclin A activity, but not cyclin A levels, was diminished in pericentrin-depleted cells compared with controls (Fig. 3c, data not shown). Similar results were obtained for several centrosome proteins (Fig. 3c). The diminished Cdk2 activity in the absence of a change in cyclin A levels suggested the presence of a Cdk inhibitory activity. In fact, human cells null for the Cdk inhibitor p21 suppressed the cell-cycle arrest (HCT116 $p21^{-/-}$, Fig. 3d), revealing a role for p21 in the inhibition of Cdk2–cyclinA complexes[19] and a molecular mechanism for the arrest.

## G1-arrested cells have defects in centrosome structure and/or organization

Because disruption of centrosome proteins induced G1 arrest from within G1, we examined G1-arrested cells for defects in centrosome structure and organization. Immunofluorescence microscopy imaging using markers for centrioles and PCM revealed three categories of structural defects: centriole loss, centriole separation and what seemed to be centriole fragments. Importantly, all centrosome protein depletions that showed cell-cycle arrest, also showed centrosome defects in one or more of these categories when compared to controls (10 out of 10).

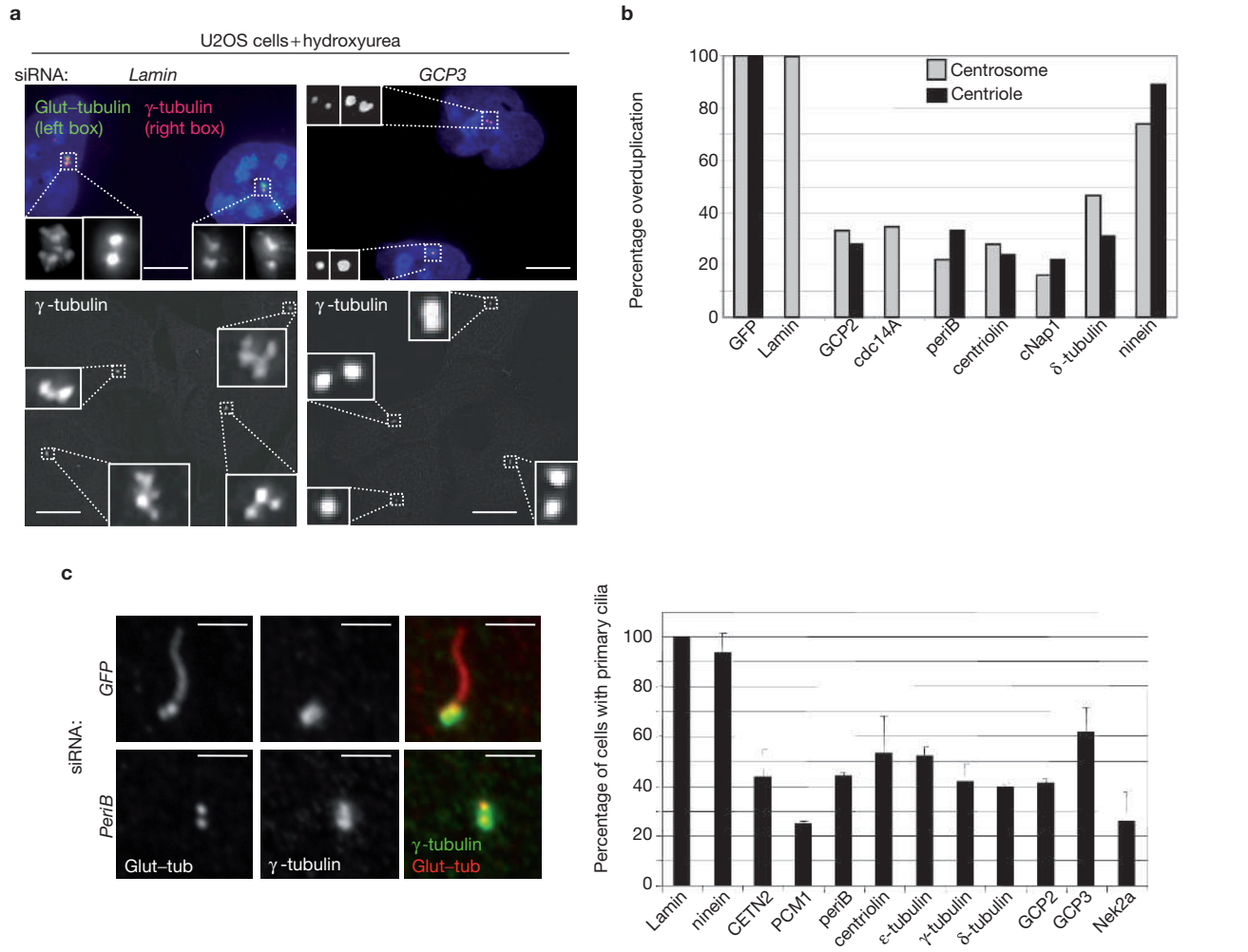


**Figure 5** G1 arrested cells exhibit defects in centrosome function. (**a**) Immunofluorescence microscopy images of centrosomes in control (*lamin* siRNA) and *GCP3*-depleted U2OS cells after treatment with hydroxyurea (48 h) to induce S-phase arrest and supernumerary centrosomes. (**b**) The histogram shows numbers of centrosomes and centrioles in hydroxyurea-treated U2OS cells after siRNA treatment (64 h) against the indicated proteins. Overduplication: >2 γ-tubulin dots (centrosome); >4 centrin dots (centrioles). $n$ = 200 cells per bar. Results are representative of three experiments. (**c**) Immunofluorescence microscopy images and quantification of primary cilia assembly in cells depleted of the indicated proteins. Cells were stained with an antibody to polyglutamylated tubulin (Glut-tub) and γ-tubulin. >200 cells per bar, normalized to 100% in control (lamin), an average of three experiments ± s.e.m. are shown. The scale bar represents 5 μm in **a** and 2 μm in **c**.

In Fig. 4A, we present data for the centrosome defect that exhibited the highest increase over control levels for each centrosome protein analysed (quantitative data for each of the three individual assays is shown in the Supplementary Information, Fig. S3). Some protein depletions induced defects in all three categories (for example, GCP2) and others in only one or two (see Supplementary Information, Fig. S3). For example, eight of nine centrosome protein depletions showed centriole loss (excluding ninein, see Supplementary Information, Fig. S3a) and six of nine showed separated centrioles (see Supplementary Information, Fig. S3b). Aberrant centrosomes did not result from cell-cycle arrest, as they were not detected in cells arrested by other means (for example, serum deprivation or hydroxyurea treatment).

The centriole-like fragments stained positively for centriole proteins (centrin) and often for a marker for stabilized tubulin (polyglutamylated tubulin), but not for PCM proteins (pericentrin and γ-tubulin, Fig. 4B). They were heterogeneous in size, usually smaller than centrioles and found in the vicinity of an intact centrosome. They were observed in four out of six centrosome protein depletions examined (see Supplementary Information, Fig. S3c). A few of the same structures were examined at higher resolution by correlative electron microscopy[20]. This revealed elements that seemed to be disorganized microtubule-like structures (Fig. 4C). Two cells had three GFP–centrin dots and all seemed to be incomplete microtubule-like structures by electron microscopy. A third cell showed no structural correlates and could represent less complete centriole structures as previously described[20]. These data suggested that centrosome-protein depletion induced formation of centriole intermediates, in addition to the original centrioles that were analogous to abnormal centrioles produced by mutation of genes involved in centriole duplication[21,22]. Taken together, the results from these three structural assays show that centrosome defects accompany G1 arrest for all centrosome depletions analysed here, suggesting a strong link between these phenotypes.

## G1-arrested cells exhibit defects in centrosome function

We reasoned that defects in centrosome structure and/or organization could perturb centrosome functions known to occur in G1, namely centrosome duplication and primary cilia assembly. In fact, previous studies

showed that loss of centrioles, as described above, was associated with improper centrosome duplication[23–25]. To examine defects in centrosome duplication, U2OS cells were treated with hydroxyurea to induce S-phase arrest and multiple rounds of centrosome duplication[26]. All centrosome protein depletions analysed that induced cell-cycle arrest and centrosome defects, also inhibited formation of supernumerary centrosomes and supernumerary centrioles (six out of six, Fig. 5a, b). In addition, supernumerary centrosomes and centrioles that occur naturally in U2OS cells (without added hydroxyurea) were reduced to more normal or lower than normal numbers (see Supplementary Information, Fig. S3d). These two assays show that centrosomes with abnormal structure were unable to duplicate properly.

We next examined the ability of centrosomes depleted of centrosome proteins to assemble primary cilia. Primary cilia are solitary microtubule-based structures that require functional centrosomes for their assembly[27], serve as environmental sensors and are implicated in human disease[28]. siRNAs targeting ten proteins that induced G1 arrest inhibited primary cilia formation (Fig. 5c). This loss of functional integrity was consistent with the observed defects in centrosome structure (Fig. 4A).

All centrosome protein depletions that lead to G1 arrest also showed defects in centrosome structure and organization, and centrosome function. This correlation is remarkable and suggests that defects in centrosome structure and function are tightly linked to centrosome-associated G1 arrest.

## G1 arrest requires p53 and p38

We next investigated regulatory molecules and pathways that could control cell-cycle progression in centrosome protein depleted cells. Immunofluorescence microscopy imaging and biochemical strategies, demonstrated that the p53 tumour suppressor accumulated in nuclei of siRNA treated cells before G1 arrest (Fig. 6a) and that p53 did not translocate to nuclei in *lamin* siRNA-treated control cells (Fig. 6a). Translocation of p53 into the nucleus is consistent with its activation[29] and indicates a role for the protein in G1 arrest. Cell lines with compromised p53 (HCT116 $p53^{-/-}$, HeLa, Saos-2; Fig. 6b and see Supplementary Information, Fig. S4a) did not undergo G1 arrest, whereas cells with wild-type p53 arrested (RPE-1, BJ-1, HME-1 and HCT-116, Figs 1, 3d).

It is possible that p53-deficient cell lines acquire additional genetic changes that contribute to cell-cycle arrest in a p53-independent manner. To overcome this potential problem, we depleted *p53* acutely using siRNAs in cells concurrently depleted of centrosome proteins and found that G1 arrest was also suppressed under these conditions (Fig. 6c and see Supplementary Information, Fig. S4b,c). p53 activation is sometimes linked to DNA damage[30], but no evidence was found for DNA damage in cells depleted of centrosome proteins using an early marker for double-strand DNA breaks, 53BP1 (ref. 31). Robust 53BP1 staining was observed when DNA was damaged by etoposide or hydroxyurea (see Supplementary Information, Fig. S4d). These results demonstrate that G1 arrest induced by centrosome protein depletion is p53-dependent and occurs without detectable DNA damage.

p53 activity is modulated by multiple signal transduction pathways[32], including p38. p38 is a member of a pathway that responds to cellular stress and is linked to the cell cycle through senescence and differentiation pathways[33]. In cells depleted of centrosome proteins, p53 was

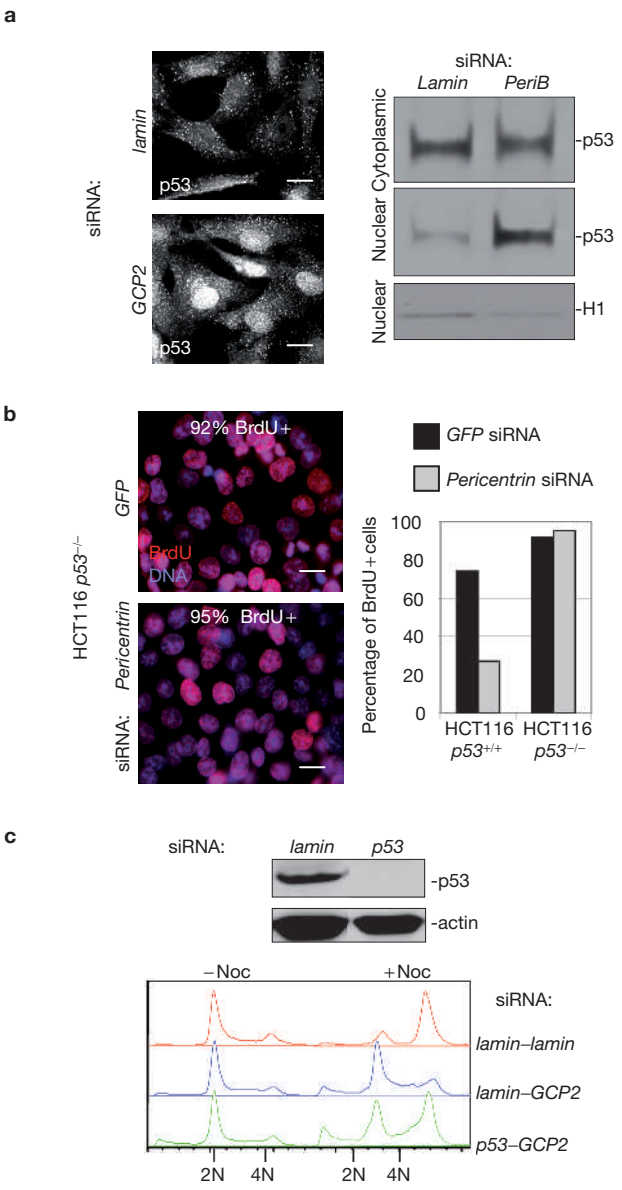


**Figure 6** G1 arrest induced by centrosome protein depletion is p53-dependent. (**a**) Immunofluorescence microscopy images showing nuclear accumulation of p53 in *GCP2* siRNA-treated cells, but not controls. Immunoblots of cytoplasmic and nuclear extracts of siRNA-treated cells showing p53 nuclear accumulation after *pericentrin* siRNA treatment, but not after *lamin* siRNA treatment. Histone H1, loading control. (**b**) Immunofluorescence microscopy images and quantification of BrdU incorporation (16 h pulse) in *pericentrin* siRNA-treated cultures (60 h) of HCT116 $p53^{-/-}$ cells. (**c**) Immunoblot from *p53* siRNA-treated and control cells. Actin, control. Flow cytometry profile of asynchronous (– noc) and nocodazole-treated (+ noc, 12 h) cells treated simultaneously with two siRNAs as indicated, >5000 cells per trace. Results are representative of at least two experiments. The scale bars represent 10 μm in **a** and **b**.

activated on Ser 33 ($p53^{P\text{-}Ser\ 33}$), a residue known to be phosphorylated by p38 (Fig. 7)[34]. This phosphorylation was not observed in *ninein*-depleted or control siRNA treated cells (Fig. 7a). Consistent with the lack of detectable DNA damage in centrosome protein-depleted cells, we did not detect phosphorylation on Ser 15 of p53 by the DNA damage-associated ATM kinase (data not shown).

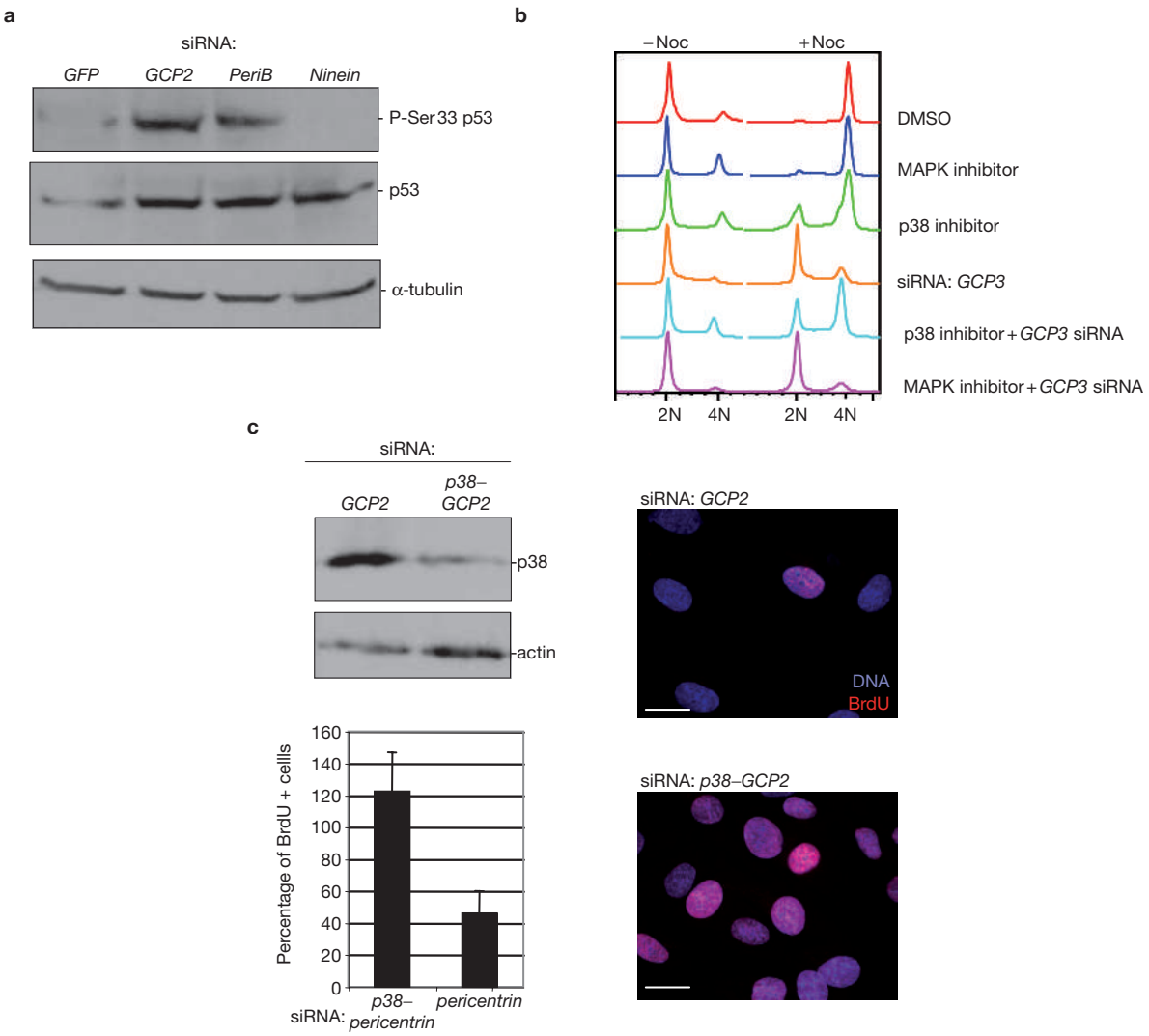


**Figure 7** G1 arrest induced by centrosome protein depletion is p38-dependent. (**a**) Immunoblot showing an increase of phospho-Ser 33 p53 in cells treated with *GCP2* and *pericentrin* siRNAs. p53 and α-tubulin were used as loading control. (**b**) Flow cytometry profiles of inhibitor-treated cells and inhibitor-treated cells depleted of *GCP3* collected in the absence or presence of nocodazole (12 h). Results are representative of three experiments, >5000 cells per trace. (**c**) Western blot showing depletion of p38. The histogram shows quantification of BrdU positive cells (normalized to untreated) after depletion of pericentrin alone, or in tandem with p38. Results are representative of three experiments and are an average of three experiments ± s.d. Immunofluorescence microscopy images show BrdU incorporation in cells depleted of *p38* and *GCP2* or *GCP2* alone. The scale bar represents 10 μm.

We next examined whether p38 was required for the centrosome associated G1 arrest. We first showed that p38 was activated in PCM1-depleted cells by its upstream kinases (MKK3/6) through phosphorylation on Thr 180 and Tyr 182 (data not shown). We next showed that SB202190 and another inhibitor of the α and β isoforms of p38 (SB203580)[35] suppressed the G1 arrest (Fig. 7b) and reduced nuclear translocation of $p53^{P\text{-}Ser\ 33}$ if added before centrosome protein depletion, but not after (data not shown). In contrast, an inhibitor of the MEK signal transduction pathway (MAPK) had no effect on cell cycling. We confirmed pharmacological suppression of the G1 arrest by siRNA-mediated depletion of *p38α* (Fig. 7c).

## The p38-activated form of p53 accumulates at centrosomes before G1 arrest

Immunofluorescence microscopy imaging demonstrated that before G1 arrest, the p38-phosphorylated form of p53 ($p53^{P\text{-}Ser\ 33}$) concentrated at centrosomes in response to centrosome protein depletion but not control protein depletion (Fig. 8a). Centrosome accumulation of $p53^{P\text{-}Ser\ 33}$ occurred before its nuclear translocation (Fig. 8a), suggesting a multistep pathway for activation and nuclear entry of p53. Activated p38 was detectable at centrosomes in mitotic and most interphase cells (Fig. 8b). In summary, we show that p38 localizes to centrosomes, that $p53^{P\text{-}Ser\ 33}$ accumulates at centrosomes specifically in response to centrosome protein depletion and that both proteins are required for the centrosome-associated cell-cycle arrest. These observations are consistent with a role for p53 and p38 in transmitting signals from the centrosome to the cell-cycle machinery (p21–cyclinA–Cdk2 complexes) as part of a cell-cycle checkpoint that monitors changes in centrosome integrity and controls G1 to S phase progression. Consistent with this model are previous studies showing that p38 activates p53 (ref. 34), that p53 activates p21 (refs 36, 37) and that p21 inhibits Cdk2–cyclin complexes[19].

## DISCUSSION

This study represents an extensive analysis of centrosome genes in vertebrate cells. We unexpectedly found that nearly all centrosome genes tested induced G1 arrest when depleted or overexpressed. Also unexpected was the observation that defects in centrosome structure and G1-centrosome functions always accompanied cell-cycle arrest, suggesting a link between these phenotypes. This work uncovers two functions common to many centrosome proteins (centrosome duplication and primary cilia assembly). We propose that these G1 functions are core functions of centrosomes in vertebrate cells. This study suggests that disruption of centrosome structure and/or function activates a 'centrosome damage' checkpoint that leads to G1 arrest.

Work from other studies supports the idea that cell-cycle progression is linked to centrosomes. Cell-cycle arrest was observed in cultured cells following centrosome disruption by laser ablation[6] or microsurgery[7], and in mouse oocytes following microinjection of centrosome antibodies[16]. Disruption of centrosome structure in all systems could logically lead to defects in centrosome functions such as duplication and primary cilia assembly, as described here. Links between premature centriole separation and aberrant centrosome duplication, and between defective centrosome duplication and cilia assembly, have been demonstrated previously[38]. Moreover, a recent paper also showed that siRNA depletion of *PCM1* and *pericentrin* induced p53-dependent cell-cycle exit[39]. Taken together, all these studies provide a strong link between defective centrosomes and cell-cycle arrest.

This study provides the first evidence for concordance between three distinct phenotypes — defective centrosome structure, centrosome dysfunction and G1 arrest. These observations provide strong support for a causal relationship between these phenotypes. We propose that cell-cycle arrest is triggered by defects in centrosome structure and/or function. Consistent with this idea, was the observation that the centrosome-bound fraction of targeted proteins was always reduced following centrosome protein depletion or expression of dominant-negative constructs. None of three phenotypes was observed following depletion of control proteins or ninein. The ability to induce G1 arrest from within G1 is consistent with disruption of centrosome and/or centriole structure and centrosome functions in G1. Finally, specific recruitment of regulatory molecules to centrosomes (p53) in response to centrosome protein depletion is consistent with a role for centrosomes in the cell-cycle arrest pathway.

The structural defects in centrosomes observed following depletion of centrosome proteins could arise through production of centrosome duplication intermediates that fail to mature, defects in parent centrosomes and/or centrioles that occur before G1, or the inability to remodel centrosomes during centrosome duplication[40]. We propose that most, if not all, centrosome proteins are required, perhaps as parts of an assembly line, to complete the construction of a functional centrosome. Master regulators likely control the overall process (for example, Plk4; refs 23, 25).

Our results suggest the presence of a novel cell-cycle checkpoint that prevents cells from entering S phase when they acquire defects in centrosome structure and/or function. Consistent with a checkpoint is the observation that centrosome-protein-depleted cells arrest with 'centrosome damage' (structural and/or functional defects) and re-enter the cell cycle only after target protein levels are restored. This mechanism of cell-cycle arrest, involving p53 recruitment to the centrosome may also apply to cells in which centrosomes have been physically altered[6,7], as these cells re-organize a functional microtubule-organizing centre that lacks centrioles but contains pericentriolar material. As with other checkpoints, cell-cycle arrest can be overcome by depleting and/or inhibiting elements of the checkpoint pathway (for example, p53, p38 and p21). Our data thus satisfy the definition of checkpoint as having three elements: a change in a condition that is sensed by the cell (altered centrosome structure and/or function), a transducing system (p38 and/or p53) and a receiver element (p21).

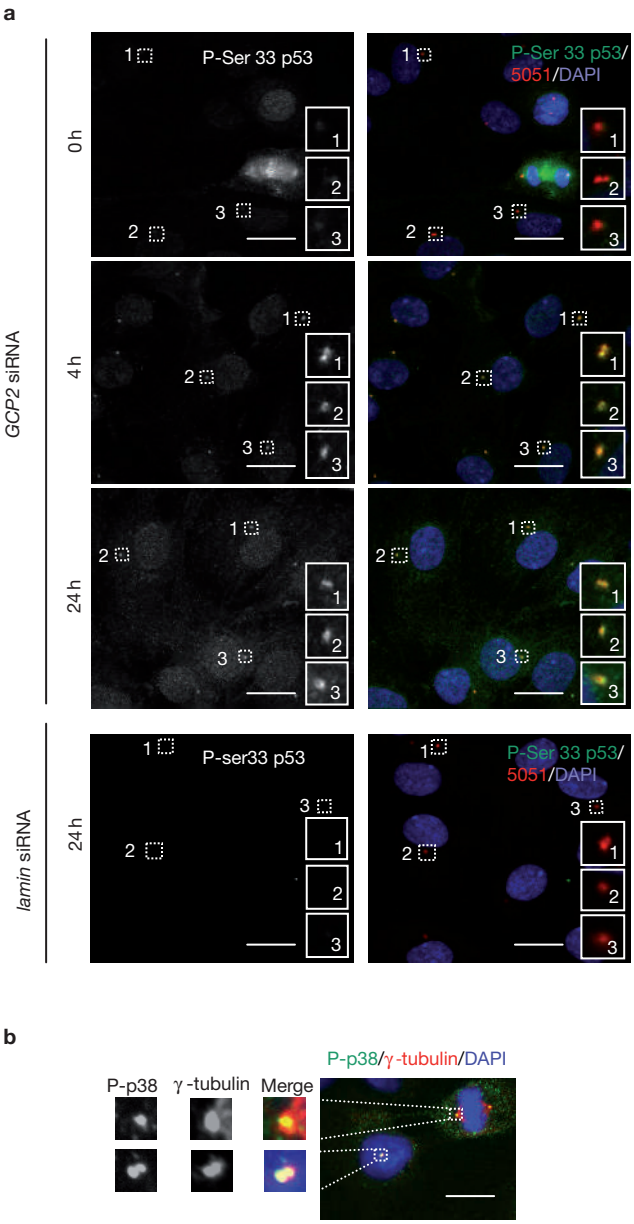


**Figure 8** The p38-activated form of p53 accumulates at the centrosome before G1 arrest. (**a**) Immunofluorescence microscopy images showing $p53^{P\text{-}Ser\ 33}$ concentrated at centrosomes in response to centrosome protein depletion (*GCP2* siRNA) 48 h after siRNA but not control protein depletion (*lamin*). Kinetic experiments (times after release from serum starvation are indicated) show p53 concentration at centrosomes (4–24 h) before the nuclear staining becomes prominent (24 h). Magnifications of the numbered boxed areas are shown in the insets. 5051, centrosome marker. (**b**) Immunofluorescence microscopy images showing phospho-p38 at the centrosome of a mitotic (top inset) and interphase cell (bottom inset). The scale bar represents 10 μm in **a** and **b**.

Abrogation of the proposed centrosome-damage checkpoint has deleterious downstream consequences. In p53-deficient HeLa cells, depletion of proteins involved in centrosome duplication induces spindle defects, cytokinesis failure and aneuploidy[24,25]. In much the same way, p53-deficiency in many human tumours may abrogate the centrosome-damage checkpoint and contribute to centrosome defects, spindle dysfunction and aneuploidy[5,41].

DNA and centrosomes are semi-conservatively replicated once every cell cycle, their replication is initiated at the same cell-cycle stage (G1) and is controlled by some similar regulatory molecules[1]. In response to DNA damage, signalling molecules such as the DNA-damage checkpoint kinase, ataxia-telangiectasia mutated (ATM) are recruited to damaged DNA. We propose that in response to centrosome damage, activated $p53^{P\text{-}Ser\ 33}$ is recruited to centrosomes. *In vivo*, the centrosome-damage checkpoint could prevent cell cycling when centrosomes are compromised by pathogens[42–44] or other external perturbations (for example, heat; data not shown)[45]. Additional studies will be required to identify other centrosome-associated molecules of the checkpoint-control pathway, to determine how p53 and p38 are anchored at centrosomes and to uncover the precise mechanism of pathway activation. □

## METHODS

**Antibodies.** We are indebted to the following investigators for providing antibodies: GCP2 and 3 (T. Stearns, Stanford, CA); ninein (G. Chan, Edmonton, Canada); Nek2a and cNap1 (A. Fry, Leicester, UK); pericentrin B (T. Davis, Seattle, WA); PCM-1 (A. Merdes, Edinburgh, UK); 20H5 Centrin-2 (J. Salisbury, Rochester, NY); cdc14A and cdc14B (P. Jackson, Stanford, CA); polyglutamylated tubulin (GT335) antibody (P. Denoulet, Paris, France); $p53^{P\text{-}Ser\ 33}$ (Y. Taya, Tokyo, Japan); and 53BP1 (T. Halazonetis, Geneva, Switzerland). Commercially available antibodies were also used: α-tubulin, γ-tubulin, ε-tubulin, actin, BrdU (Sigma, St Louis, MO); Ki-67 (BD Biosciences, Franklin Lakes, NJ); lamin A/C (Cell Signaling, Boston, MA); p38, histone H1, zyxin, Nek2, δ-tubulin, ε-tubulin (Santa Cruz Biotechnology, Santa Cruz, CA); phospho-p38 (Thr180/Tyr182, Cell Signaling); p53 (ab-2), p53 (ab-6). Pericentrin $A/B^{27}$ 5051 (ref. 46) and cyclins A2, B1, cdk1-2 (ref. 47) have been described previously.

**Cell culture, siRNA, transfection and microinjection.** These studies primarily used diploid, telomerase-immortalized RPE-1 cells (Clontech, Mountain View, CA)[48], cell lines containing wild-type p53 (BJ-1, HCT116, IMR-90, HCT116 $p21^{-/-}$) or compromised p53 (Saos-2, HeLa, HCT116 $p53^{-/-}$; HCT116 series, generous gift from B. Vogelstein, Baltimore, MD). HeLa and U2OS stably expressing GFP–centrin2 were prepared in our laboratory. Cells were grown as described by American Type Culture Collection (Manassas, VA). For G0–G1 synchrony, cells were grown for 24 h in media with reduced serum (0.25%) before experimentation. Targeted proteins were depleted with siRNAs delivered to cells at 1–200 nM using Oligofectamine or Lipofectamine 2000 (Invitrogen, Carlsbad, CA) per manufacturers instructions. Synthetic double-stranded siRNAs (Dharmacon, Lafayette, CO) were designed according to recently published suggestions[48] (for siRNA sequences see Supplementary Information, Fig. S1e). For rescue experiment siRNA, Smart pool siRNA localized in the UTR region was purchased from Dharmacon. Several genes were targeted with a second siRNA to eliminate possible non-specific effects. p38 (SB202190; Calbiochem, La Jolla, CA) and MAPK (PD98059) inhibitors were used at 10 μM and 50 μM respectively. For telophase microinjection experiments, cells synchronized in mitosis by 10 h nocodazole incubation (0.5 μg $ml^{-1}$), were microinjected into the nucleus 1 h after release, with either a plasmid encoding $RFP\text{–}Peri^{CT}$, or a control RFP plasmid using an Eppendorf transjector 5246 and Micromanipulator (Brinkman, Westbury, NY). Immediately after microinjection, cells were incubated with 10 μM BrdU for 24 h before fixation and staining. Alternatively, cells were transfected using calcium phosphate and incubated for 24 h with BrdU followed by fixation and staining.

**Immunofluorescence microscopy and immunoblotting.** Cells were prepared for immunofluorescence microscopy, imaged, deconvolved (Meta-Morph; Universal Imaging Corp., Downington, PA), displayed as two-dimensional projections of three-dimensional reconstructions to visualize the entire cell volume, and quantified as previously described[8]. Pixel intensity profiles (total intensity plot) were constructed from maximal intensity projections using Meta-Morph. Crude cell lysates were analysed for protein depletion. Cells were treated with siRNAs for 48–72 h, harvested and lysed in PBS supplemented with 1% Triton X-100 and a cocktail of protease inhibitors. Cell lysates were clarified at top speed in a microfuge for 15 min at 5 °C. Protein concentration for each lysate was determined using Bio-Rad protein dye reagent, loads were adjusted and proteins were resolved by SDS–PAGE and analysed by western blot. Uncropped images of key western blots are shown in the Supplementary Information, Fig. S5.

**Kinase assays and nuclear fractions.** Immunoprecipitations and kinase assays were performed as previously described[47]. Affinity-purified cyclin A antibodies were cross-linked to Sepharose beads and incubated with cell lysates (100–300 μg proteins) for 3 h before being washed four times in buffer. Precipitated proteins were resuspended in 20 μl 1× SDS–PAGE sample buffer for immunoblot analysis. For kinase assays, immunoprecipitation beads were dissolved in 5 μl kinase buffer with 10 mM DTT and 20–50 μM ATP. Each sample was incubated with 5–10 μCi $\gamma\text{-}^{32}$P-ATP (#BLU-502A; PE/NEN Life Sciences, Boston, MA) and 1.5 μg histone H1 (#1004875; Roche, Basel, Switerland) in a final volume of 16 μl for 30 min at 30 °C. Reactions were terminated with 8 μl 5× SDS–PAGE sample buffer and processed for autoradiography and quantified by phosphorimage analysis (Storm 820, Molecular Probes, Carlsbad, CA). Nuclear fractions were prepared by resuspending trypsinized cells in cold nuclear extraction buffer (320 mM sucrose, 5 mM $MgCl_2$, 10 mM HEPES, 1% Triton X-100 at pH 7.4) by gentle vortexing, followed by incubation on ice for 10 min. Nuclei were then pelleted at 2,000*g* and washed twice with nuclei extraction buffer without Triton X-100. Nuclei yield and integrity were confirmed by microscopic examination. All washes were combined to obtain the cytoplasmic fraction and both fractions were processed for immunoblot analysis (as above).

**Flow cytometry, BrdU assay and proliferation assay.** Cells treated with siRNAs for 48–72 h were exposed to 1–5 μg $ml^{-1}$ nocodazole for 12 h, removed from plates and fixed in ethanol. Cells stained with propidium iodide were analysed by flow cytometry (FACSCAN, Becton Dickinson, Franklin Lakes, NY) using FlowJo software (Tree Star, Inc., Ashland, OR). BrdU labelling was performed essentially as previously described[49]. Cells were incubated with 10 μM BrdU for 16–24 h before fixation in 4% formaldehyde for 2 min and post-fixation in 100% methanol. Generational tracking of cell populations by flow cytometry was accomplished by labelling cellular proteins with 2 μM carboxyfluoroscein diacetate, succinimidyl ester (CFDA-SE, Molecular Probes) for 5 min according to the manufacturers' specifications, so that each cell division results in halving of the total cellular fluorescence.

**Centrosome duplication, primary cilia formation and quantification of centrosome defects.** After 24 h of siRNA-mediated depletion of centrosome proteins, U2OS cells were blocked in S-phase by incubation in hydroxyurea-containing growth media (4 mM) for an additional 40 h before fixation in 100% ice-cold methanol. To unambiguously identify centrioles in interphase, cells were pre-treated with nocodazole (5 μg $ml^{-1}$) for 2 h or incubated on ice for 30 min to depolymerize microtubules before fixation. Centrioles from untreated U2OS cells in interphase and mitosis were also counted. The indicated antibodies were used to detect centrosomes and centrioles. Primary cilia were detected as described using GT335 antibody[27]. Briefly, cells were retransfected 48 h after the first siRNA transfection using Oligofectamine. At 72 h, primary cilia were induced by culturing RPE1 cells in medium with 0.25% serum for 48 h. To quantify centrosome defects (Fig. 4A), three categories of centrosome defects were an analysed (structure, separation and loss). For each depleted centrosome protein, the assay showing the largest difference compared with control was plotted as the fold difference and compared with ninein.

*Note: Supplementary Information is available on the Nature Cell Biology website.*

ACKNOWLEDGEMENTS

We thank B. Theurkauf, D. McCollum, C. Sherr and C. Havens for useful discussions on this work. This work was supported by funding from the National Institutes of Health (GM51994) to S.J.D., the Department of Defense to K.M., B.D. (DMAD17-03-1-0303) and A.J. (DAMD17-03-1-056), and the Intramural Research Program of the National Cancer Institute (P.K.).

## AUTHOR CONTRIBUTIONS

This project was conceived, planned and much of it executed by K.M. Much of the quantitative data on centrosome function and structure and the rescue experiments were performed by B.D. P.K. peformed the Cdk–cyclin immunoprecipitations and assays, and P.H. performed electron microscopy.

## COMPETING INTEREST STATEMENT

The authors declare that they have no competing financial interests.

Published online at http://www.nature.com/naturecellbiology/
Reprints and permissions information is available online at http://npg.nature.com/reprintsandpermissions/

1. Doxsey, S., Zimmerman, W. & Mikule, K. Centrosome control of the cell cycle. *Trends Cell Biol.* **15,** 303–311 (2005).
2. Hinchcliffe, E. H. & Sluder, G. "It takes two to tango": understanding how centrosome duplication is regulated throughout the cell cycle. *Genes Dev.* **15,** 1167–1181 (2001).
3. Lacey, K. R., Jackson, P. K. & Stearns, T. Cyclin-dependent kinase control of centrosome duplication. *Proc. Natl Acad. Sci. USA* **96,** 2817–2822 (1999).
4. Pihan, G. A. *et al.* Centrosome defects and genetic instability in malignant tumors. *Cancer Res.* **58,** 3974–3985 (1998).
5. Nigg, E. A. Centrosome aberrations: cause or consequence of cancer progression? *Nature Rev. Cancer* **2,** 815–825 (2002).
6. Khodjakov, A. & Rieder, C. L. Centrosomes enhance the fidelity of cytokinesis in vertebrates and are required for cell cycle progression. *J. Cell Biol.* **153,** 237–242 (2001).
7. Hinchcliffe, E. H., Miller, F. J., Cham, M., Khodjakov, A. & Sluder, G. Requirement of a centrosomal activity for cell cycle progression through G1 into S phase. *Science* **291,** 1547–1550 (2001).
8. Gromley, A. *et al.* A novel human protein of the maternal centriole is required for the final stages of cytokinesis and entry into S phase. *J. Cell Biol.* **161,** 535–545 (2003).
9. Wong, C. & Stearns, T. Mammalian cells lack checkpoints for tetraploidy, aberrant centrosome number, and cytokinesis failure. *BMC Cell Biol.* **6,** 6 (2005).
10. Uetake, Y. & Sluder, G. Cell cycle progression after cleavage failure: mammalian somatic cells do not possess a "tetraploidy checkpoint". *J. Cell Biol.* **165,** 609–615 (2004).
11. Matsumoto, Y. & Maller, J. L. A centrosomal localization signal in cyclin E required for Cdk2-independent S phase entry. *Science* **306,** 885–888 (2004).
12. Gerdes, J. *et al.* Cell cycle analysis of a cell proliferation-associated human nuclear antigen defined by the monoclonal antibody Ki-67. *J. Immunol.* **133,** 1710–1715 (1984).
13. Delgehyr, N., Sillibourne, J. & Bornens, M. Microtubule nucleation and anchoring at the centrosome are independent processes linked by ninein function. *J. Cell Sci.* **118,** 1565–1575 (2005).
14. Casenghi, M. *et al.* Polo-like kinase 1 regulates Nlp, a centrosome protein involved in microtubule nucleation. *Dev. Cell* **5,** 113–125 (2003).
15. Gillingham, A. K. & Munro, S. The PACT domain, a conserved centrosomal targeting motif in the coiled-coil proteins AKAP450 and pericentrin. *EMBO Rep.* **1,** 524–529 (2000).
16. Balczon, R., Simerly, C., Takahashi, D. & Schatten, G. Arrest of cell cycle progression during first interphase in murine zygotes microinjected with anti-PCM-1 antibodies. *Cell Motil. Cytoskeleton* **52,** 183–192 (2002).
17. Gromley, A. *et al.* Centriolin anchoring of exocyst and SNARE complexes at the midbody is required for secretory-vesicle-mediated abscission. *Cell* **123,** 75–87 (2005).
18. Nose, A. & Takeichi, M. A novel cadherin cell adhesion molecule: its expression patterns associated with implantation and organogenesis of mouse embryos. *J. Cell Biol.* **103,** 2649–2658 (1986).
19. Sherr, C. J. & Roberts, J. M. CDK inhibitors: positive and negative regulators of G1-phase progression. *Genes Dev.* **13,** 1501–1512 (1999).
20. La Terra, S. *et al.* The *de novo* centriole assembly pathway in HeLa cells: cell cycle progression and centriole assembly/maturation. *J. Cell Biol.* **168,** 713–722 (2005).
21. Kirkham, M., Muller-Reichert, T., Oegema, K., Grill, S. & Hyman, A. A. SAS-4 is a C. elegans centriolar protein that controls centrosome size. *Cell* **112,** 575–587 (2003).
22. Leidel, S. & Gonczy, P. SAS-4 is essential for centrosome duplication in *C. elegans* and is recruited to daughter centrioles once per cell cycle. *Dev. Cell* **4,** 431–439 (2003).
23. Habedanck, R., Stierhof, Y. D., Wilkinson, C. J. & Nigg, E. A. The Polo kinase Plk4 functions in centriole duplication. *Nature Cell Biol.* **7,** 1140–1146 (2005).
24. Salisbury, J. L., Suino, K. M., Busby, R. & Springett, M. Centrin-2 is required for centriole duplication in mammalian cells. *Curr. Biol.* **12,** 1287–1292 (2002).
25. Bettencourt-Dias, M., *et al.* SAK/PLK4 is required for centriole duplication and flagella development. *Curr. Biol.* **15,** 2199–2207 (2005).
26. Balczon, R. *et al.* Dissociation of centrosome replication events from cycles of DNA synthesis and mitotic division in hydroxyurea-arrested Chinese hamster ovary cells. *J. Cell Biol.* **130,** 105–115 (1995).
27. Jurczyk, A. *et al.* Pericentrin forms a complex with intraflagellar transport proteins and polycystin-2 and is required for primary cilia assembly. *J. Cell Biol.* **166,** 637–643 (2004).
28. Pazour, G. J. & Witman, G. B. The vertebrate primary cilium is a sensory organelle. *Curr. Opin. Cell Biol.* **15,** 105–110 (2003).
29. Rubbi, C. P. & Milner, J. Disruption of the nucleolus mediates stabilization of p53 in response to DNA damage and other stresses. *EMBO J.* **22,** 6068–6077 (2003).
30. Zhan, Q., Carrier, F. & Fornace, A. J., Jr. Induction of cellular p53 activity by DNA-damaging agents and growth arrest. *Mol. Cell Biol.* **13,** 4242–4250 (1993).
31. Wang, B., Matsuoka, S., Carpenter, P. B. & Elledge, S. J. 53BP1, a mediator of the DNA damage checkpoint. *Science* **298,** 1435–1438 (2002).
32. Wu, G. S. The functional interactions between the p53 and MAPK signaling pathways. *Cancer Biol. Ther.* **3,** 156–161 (2004).
33. Yee, A. S. *et al.* The HBP1 transcriptional repressor and the p38 MAP kinase: unlikely partners in G1 regulation and tumor suppression. *Gene* **336,** 1–13 (2004).
34. Kishi, H. *et al.* Osmotic shock induces G1 arrest through p53 phosphorylation at Ser33 by activated p38MAPK without phosphorylation at Ser15 and Ser20. *J. Biol. Chem.* **276,** 39115–39122 (2001).
35. Lee, J. C. *et al.* A protein kinase involved in the regulation of inflammatory cytokine biosynthesis. *Nature* **372,** 739–746 (1994).
36. Harper, J. W., Adami, G. R., Wei, N., Keyomarsi, K. & Elledge, S. J. The p21 Cdk-interacting protein Cip1 is a potent inhibitor of G1 cyclin-dependent kinases. *Cell* **75,** 805–816 (1993).
37. el-Deiry, W. S. *et al.* WAF1, a potential mediator of p53 tumor suppression. *Cell* **75,** 817–825 (1993).
38. Dutcher, S. K. Elucidation of basal body and centriole functions in *Chlamydomonas reinhardtii*. *Traffic* **4,** 443–451 (2003).
39. Srsen, V., Gnadt, N., Dammermann, A. & Merdes, A. Inhibition of centrosome protein assembly leads to p53-dependent exit from the cell cycle. *J. Cell Biol.* **174,** 625–630 (2006).
40. Leidel, S., Delattre, M., Cerutti, L., Baumer, K. & Gonczy, P. SAS-6 defines a protein family required for centrosome duplication in C. elegans and in human cells. *Nature Cell Biol.* **7,** 115–125 (2005).
41. Pihan, G. A. *et al.* Centrosome defects can account for cellular and genetic changes that characterize prostate cancer progression. *Cancer Res.* **61,** 2212–2219 (2001).
42. Grieshaber, S. S., Grieshaber, N. A., Miller, N. & Hackstadt, T. *Chlamydia trachomatis* causes centrosomal defects resulting in chromosomal segregation abnormalities. *Traffic* **7,** 940–949 (2006).
43. Ploubidou, A. *et al.* Vaccinia virus infection disrupts microtubule organization and centrosome function. *EMBO J.* **19,** 3932–3944 (2000).
44. Jouvenet, N. & Wileman, T. African swine fever virus infection disrupts centrosome assembly and function. *J. Gen. Virol.* **86,** 589–594 (2005).
45. Vidair, C. A., Doxsey, S. J. & Dewey, W. C. Thermotolerant cells possess an enhanced capacity to repair heat-induced alterations to centrosome structure and function. *J. Cell. Physiol.* **163,** 194–203 (1995).
46. Tuffanelli, D. L., McKeon, F., Kleinsmith, D. M., Burnham, T. K. & Kirschner, M. Anticentromere and anticentriole antibodies in the scleroderma spectrum. *Arch. Dermatol.* **119,** 560–566 (1983).
47. Berthet, C., Aleem, E., Coppola, V., Tessarollo, L. & Kaldis, P. Cdk2 knockout mice are viable. *Curr. Biol.* **13,** 1775–1785 (2003).
48. Morales, C. P. *et al.* Absence of cancer-associated changes in human fibroblasts immortalized with telomerase. *Nature Genet.* **21,** 115–118 (1999).
49. Kennedy, B. K., Barbie, D. A., Classon, M., Dyson, N. & Harlow, E. Nuclear organization of DNA replication in primary mammalian cells. *Genes Dev.* **14,** 2855–2868 (2000).

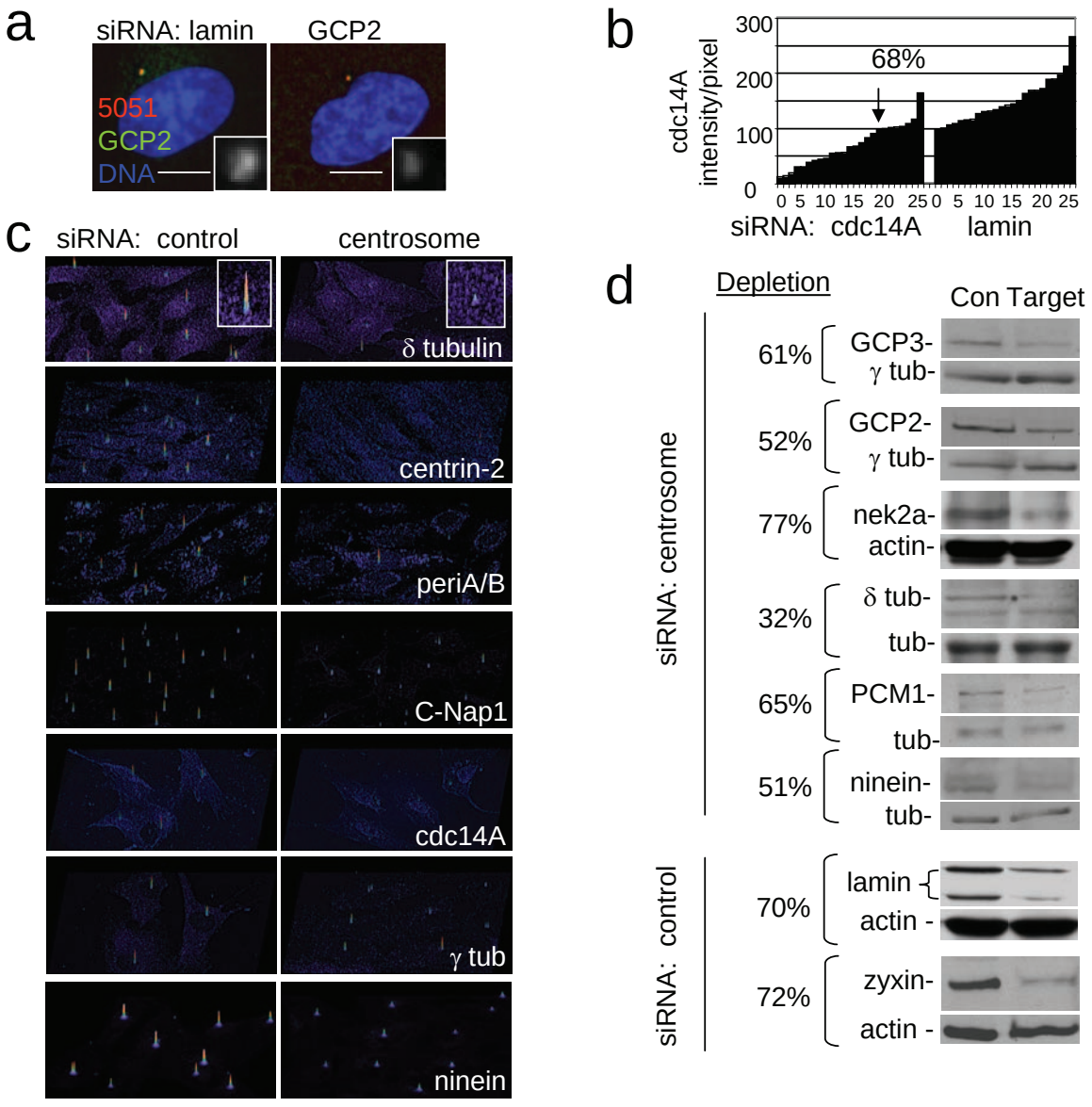

e

**Control siRNA sequences used:**

| | |
|---|---|
| GFP | CAUGAAGCAGCACGACUUC |
| LAMIN A/C | CUGGACUUCCAGAAGAACA |
| KER18 | CAUCAAGGUCAAGCUGGAC |
| ZYXIN | UGUGGCUGUCAACGAACUC |

**Centrosome protein siRNA sequences used:**

| | | |
|---|---|---|
| CENTRIOLIN | GGAUCAGAGACUCUACCUU | |
| PERI A/B | GAAGGAGAAGGAGACGGCA | |
| PERI A/B.2 | GCAGCUGAGCUGAAGGAGA | **(Shown throughout paper)** |
| PERI B | UUGGAACAGCUGCAGCAGA | **(Shown throughout paper)** |
| NINEIN | GUGCUGCAGCAGACAUUAC | |
| NINEIN.2 | UAUGAGCAUUGAGGCAGAG | |
| GAMMA | UGACCGCAAGGACGUCUUU | |
| GCP2 | UCUCGUACUCCAGAAGACU | |
| GCP2.2 | AGAUCGAGAAGGCGUUUAA | |
| GCP3 | UGCAGCAUCUGCUUCUCUU | |
| GCP5 | ACUUCGCCUGGUCCAACUU | |
| CNAP1 | UCUAUCCGAAAGCCCAGUC | |
| CNAP1.2 | CUGUCACUCAAGCCAAGGA | |
| PCM1 | GUCCCCCAAACAGAGAAAC | |
| PCM1.2 | UCAGCUUCGUGAUUCUCAG | |
| DELTA TUB | GGUUCUGGAAACAACUGGG | |
| NEK2 | AGGGAACCAAGGAAAGGCA | |
| EPSILON TUB | AGUCGGCAGAGCACUGUGA | |
| CDC14A | GCACAGUAAAUACCCACUA | |
| CDC14A.2 | CCGUGCGUAUCUCGCUUAA | |
| CDC14B | GCAAAUGCUGCCUUCCUUG | |
| CENTRIN2 | GAGCAAAAGCAGGAGAUCC | **(Shown in Figure 2)** |
| CENTRIN2 | SmartPOOL UTR region | **(Shown in Figure 2)** |

**Other siRNA sequences used:**

| | |
|---|---|
| P53 | GGACAAGGGUUGGGCUGGG |
| P53.2 | AGACUCCAGUGGUAAUCUA |
| P38 | UGUGAUUGGUCUGUUGGAC |
| P38.2 | CCAAAUUCUCCGAGGUCUA |

**Figure S1** siRNAs specifically deplete centrosomal proteins. **a,** Immunofluorescence images show reduction of GCP2 protein at the centrosome 72h after GCP2 siRNA treatment compared to control (lamin). Inset : 5X magnification of centrosomal GCP2 signal. 5051, centrosome marker. Scale bar: 5µm **b,** Graph displays the average fluorescence intensity/pixel of cdc14A at individual centrosomes (bars) in siRNA-treated cells (72h). Arrow shows that 68% of cdc14A siRNA-treated cultures are below the lowest control levels. **c,** Semi-quantitative pixel intensity profiles, constructed from optically sectioned (Z-axis) fluorescence images of cells treated with siRNAs targeting lamin (left, control) or centrosomal proteins (right, as indicated), shows that siRNAs deplete targeted proteins at the centrosomes . **d,** Western blots from siRNA-treated cultures (72h) probed for the targeted protein (Target) or control (Con, usually lamin), as indicated. Actin, γ tubulin, or pan-specific tubulin immunoblots demonstrate equivalent loading conditions as indicated (lower panels of each set). **e,** siRNAs sequences used to target centrosome proteins. Underlined sequences are presented in the paper.

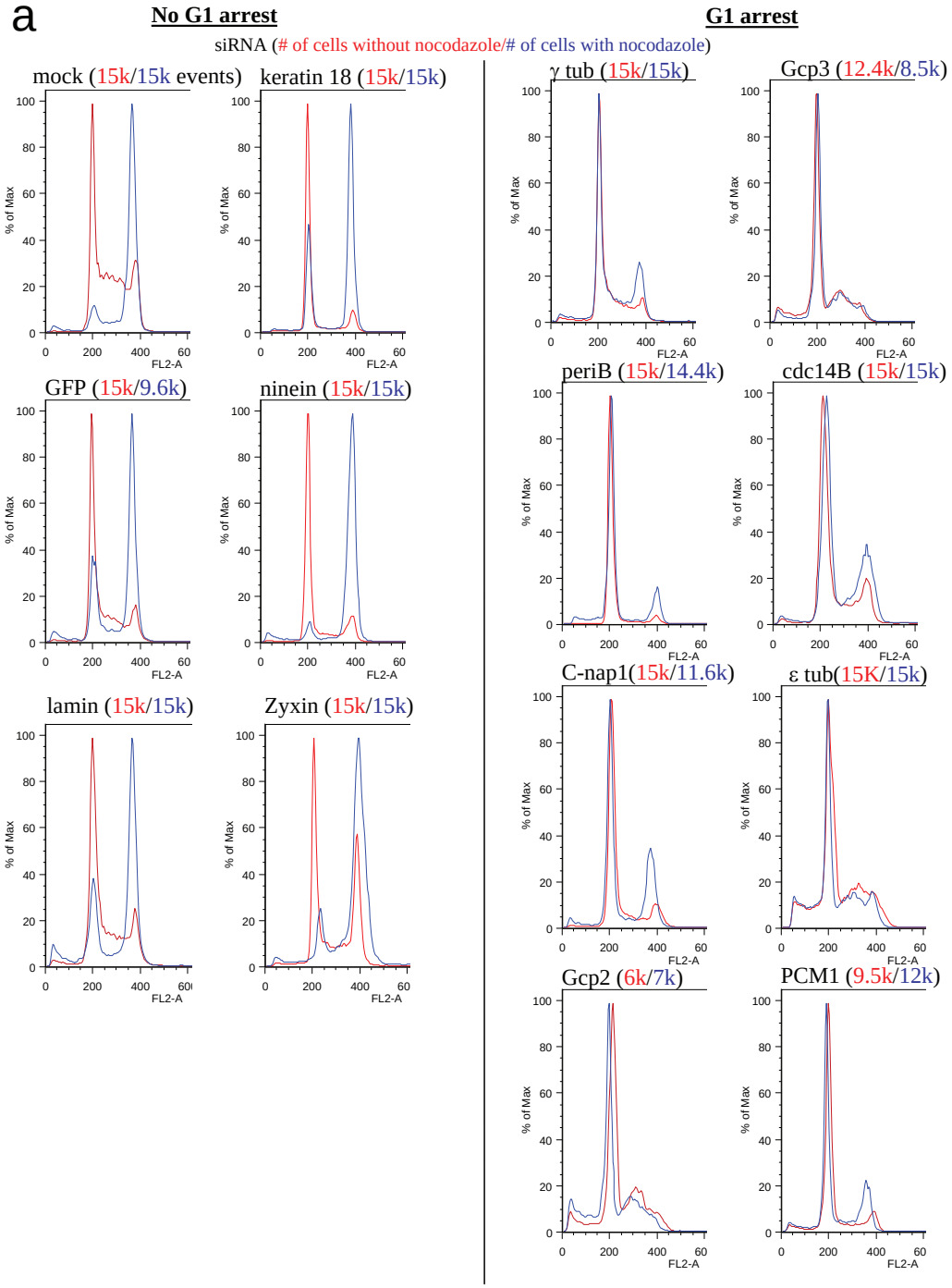

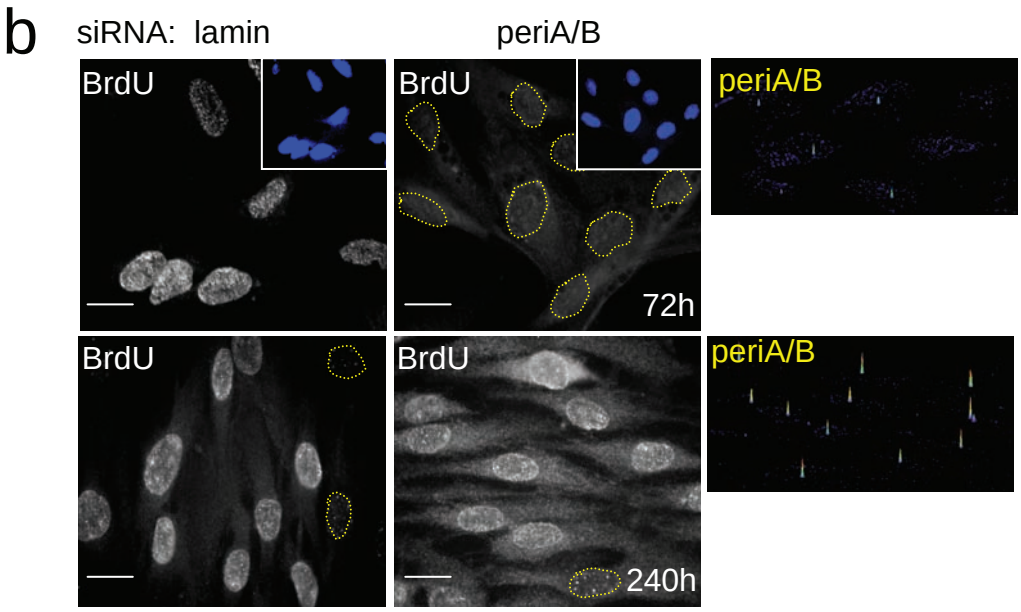


**Figure S2** **a,** Cell cycle arrest is induced after centrosome protien depletion. Flow cytometry traces of RPE cells treated with indicated siRNAs. Red, no nocodazole; blue, + nocodazole. The number of cells examined are shown in parentheses where the colors indicate -noc/+noc. See Fig.1 for details. **b,** Cell cycle arrest induced by pericentrin depletion (periA/B, 72h, upper panel) is relieved upon return to normal protein levels (periA/B, 240h, lower panel). BrdU incorporation in cells treated with lamin or pericentrin-specific siRNAs for 72 or 240 hours. Centrosome pixel intensity profiles (right panels) show that centrosomal levels of pericentrin returns to normal (top) when cells begin cycling and incorporate BrdU. Scale bar: 10μm. Insets: DAPI stain. Dotted lines: nucleus.

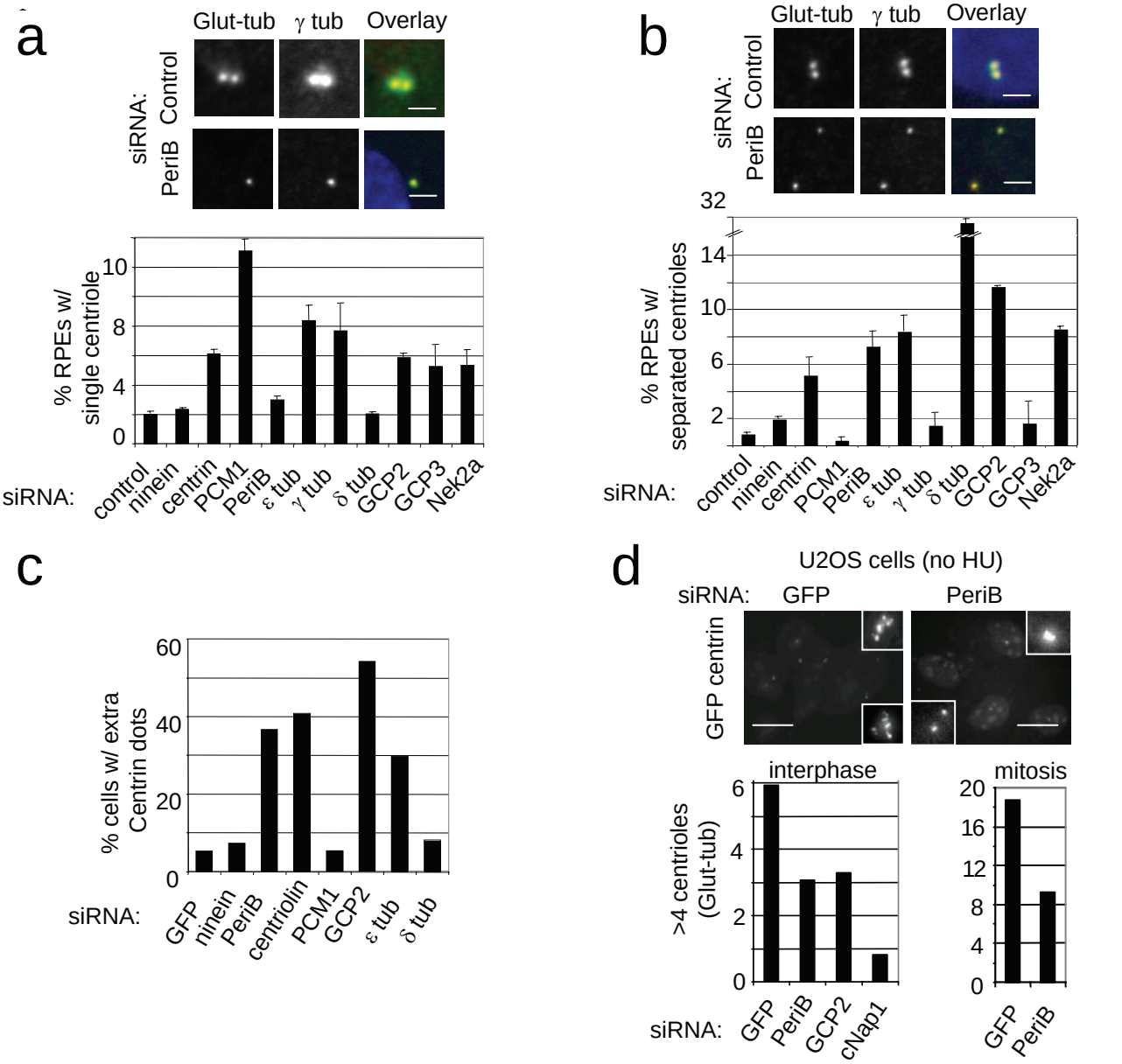


**Figure S3** Structural and functionnal defects induced in RPE cells after centrosome protein depletion. **a,** Immunofluorescence images and quantification of RPE cells with single centriole (stained with polyglutamylated-tubulin, Glut-tub) after siRNA-depletion of the indicated proteins and serum withdrawal. Scale bar: 2µm. Average of 2 experiments ± SEM. >200 cells /bar. **b,** Immunofluorescence images and quantification of RPE cells with separated centrioles (stained with Glut-tub) after siRNA-depletion of the indicated proteins and serum withdrawal. Scale bar: 2µm. Average of 2 experiments ± SEM. >200 cells /bar. **c,** Quantification of GFP-centrin expressing RPE cells with extra GFP-centrin structures (presumed centriole intermediates) induced in RPE cells after siRNA treatment as indicated. >200 cells/bar. **d,** Defects in centrosome duplication leads to reduction of centriole number in U2OS cells in the absence of hydroxyurea (HU). Immunofluorescence images of centrosomes in control (GFP siRNA) and periB siRNA-depleted non-hydroxyurea-treated U2OS cells showing centriole number reduction (GFP-centrin). Quantification of centriole reduction (Glut-tub) in interphase (left) and mitotic (right) U2OS cells following siRNA treatment of the indicated proteins. Scale bar: 10µm. >100 interphase cells or >150 mitotic cells/ bar.

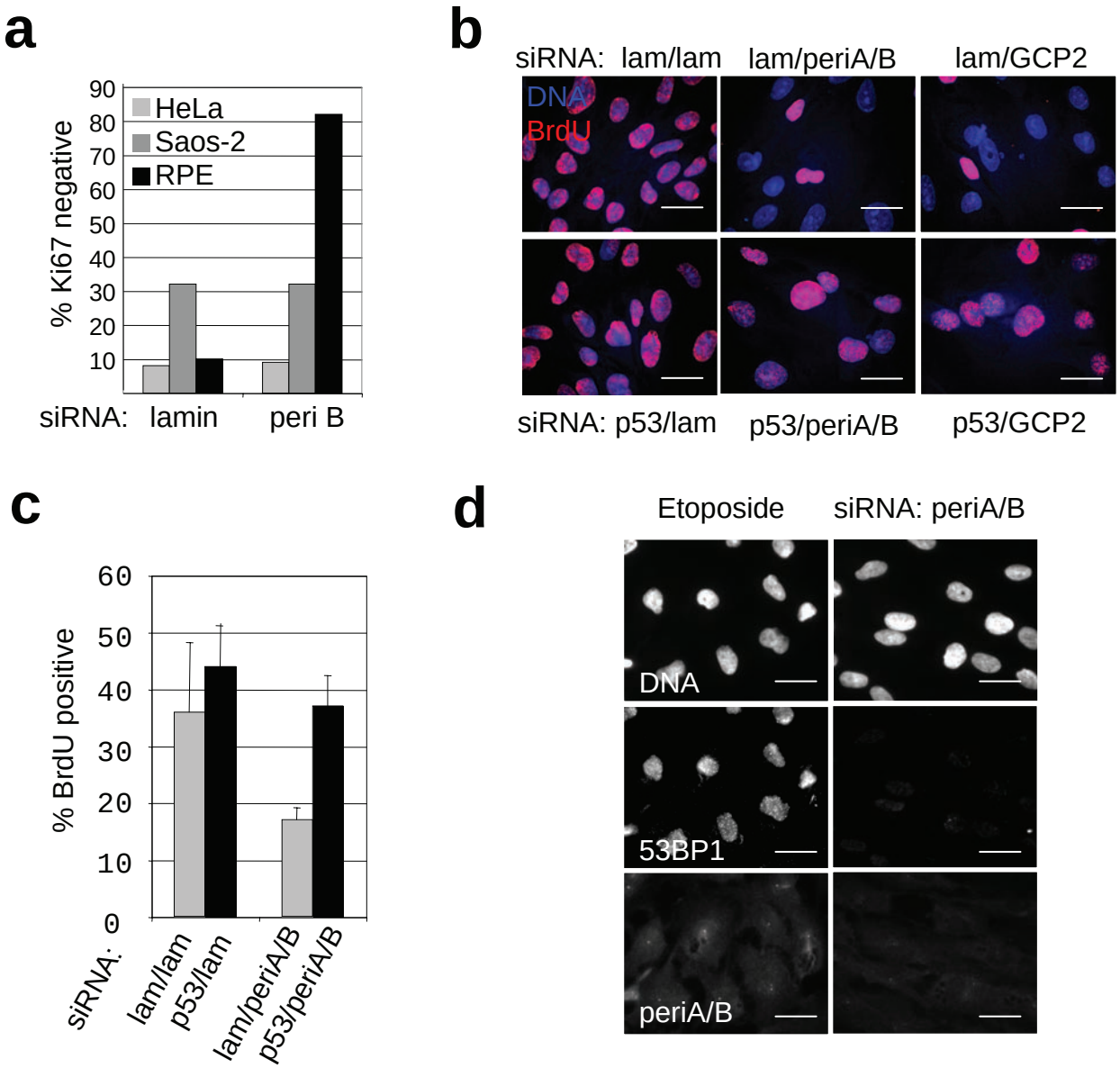


**Figure S4** G1 arrest is p53-dependent and occurs without detectable DNA damage. **a,** p53-deficient cells (HeLa, Saos) do not arrest. Graph shows percentage of Hela, Saos-2, and RPE cells staining negatively for Ki67 following depletion of lamin or pericentrin B (peri B). n=1000 cells/bar **b,** p53 depletion suppresses cell cycle arrest in RPE cells. BrdU incorporation in cells pretreated with siRNAs directed against either lamin or p53 for 24h, then treated with indicated siRNA (after backslash) for 72 hour. BrdU was added 24h before processing. Scale bar: 10μm. **c,** Quantification of cell cycle arrest suppression after p53 depletion. BrdU incorporation in cells pretreated with siRNAs directed against either lamin or p53 for 24h, then treated with siRNA (after backslash: lam, periA/B). Average of 3 experiments +/- SD. **d,** Cell cycle arrest occurs without detectable DNA damage. p53BP1 is not affected following centrosome protein depletion. Cell cultures treated with either etoposide (positive control) or pericentrin depleted cells were stained with an antibody directed against p53BP1, to reveal damaged DNA. Co-staining of pericentrin (periA/B) included to show specificity of protein depletion. Scale bar: 10μm.

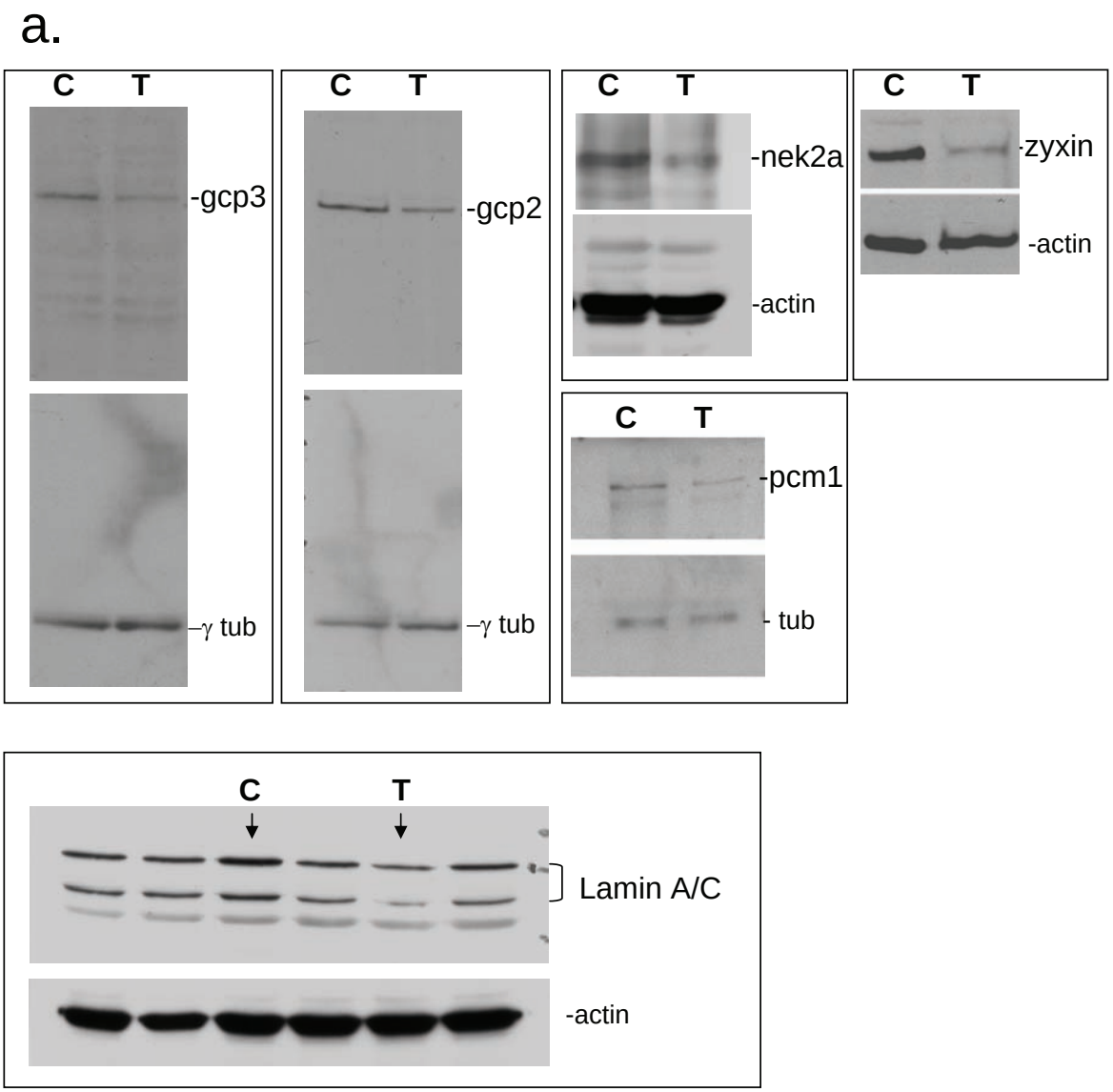


**Figure S5** Western blots shown in full **a,** Western blots from Supplemental Fig1. C: control siRNA, T: target siRNA **b,** Western blots from Fig. 3c. **c,** Western blots from Fig. 6c . **d,** Western blots from Fig 7a. **e,** Western blots from Fig. 7c. C: control siRNA, T: target siRNA